Journal of Power Sources 193 (2009) 447–453

Contents lists available at ScienceDirect

Journal of Power Sources

journal homepage: www.elsevier.com/locate/jpowsour

Membrane electrode assembly with doped polyaniline interlayer for proton exchange membrane fuel cells under low relative humidity conditions

L. Cindrella[a,b], A.M. Kannan[a,*]

[a] Fuel Cell Research Lab, Engineering Technology Department, Arizona State University, Mesa, AZ 85212, USA
[b] Department of Chemistry, National Institute of Technology, Tiruchirappalli, Tamil Nadu 620015, India

ARTICLE INFO

Article history:
Received 2 February 2009
Received in revised form 28 March 2009
Accepted 9 April 2009
Available online 17 April 2009

Keywords:
Polyaniline
Membrane electrode assembly
Surface morphology
PEM fuel cells

ABSTRACT

A membrane electrode assembly (MEA) was designed by incorporating an interlayer between the catalyst layer and the gas diffusion layer (GDL) to improve the low relative humidity (RH) performance of proton exchange membrane fuel cells (PEMFCs). On the top of the micro-porous layer of the GDL, a thin layer of doped polyaniline (PANI) was deposited to retain moisture content in order to maintain the electrolyte moist, especially when the fuel cell is working at lower RH conditions, which is typical for automotive applications. The surface morphology and wetting angle characteristics of the GDLs coated with doped PANI samples were examined using FESEM and Goniometer, respectively. The surface modified GDLs fabricated into MEAs were evaluated in single cell PEMFC between 50 and 100% RH conditions using H_2 and O_2 as reactants at ambient pressure. It was observed that the MEA with camphor sulfonic acid doped PANI interlayer showed an excellent fuel cell performance at all RH conditions including that at 50% at 80 °C using H_2 and O_2.

1. Introduction

Proton exchange membrane fuel cells (PEMFCs) are promising alternative power sources for various applications due to their higher power densities and environmental benefits. However, the power density values are reduced due to mass transport limitations mainly at the cathode, when air is used. To improve the performance of the PEMFCs, it is critical to balance the properties of the gas flow characteristics in the membrane electrode assembly (MEA). Gas diffusion layer (GDL) is one of the critical components of a fuel cell that has the ability to influence the performance at high current density region. The water retaining (hydrophilicity) and water expelling (hydrophobicity) properties of the GDLs have to be watchfully balanced to achieve optimum performance of the fuel cell without flooding when it operates under 100% relative humidity (RH) conditions of reactant gases [1–6]. The hydrophilicity of the gas diffusion layers can also avoid drying of electrolyte in lower RH conditions. In general, GDLs are fabricated by coating a macro-porous layer (carbon paper or carbon cloth) with hydrophobic micro-porous layer. Many strategies are currently emerging to design and develop purpose-built GDLs incorporating various carbon materials for specific operating conditions of fuel cells [7–11]. This is achieved through manifestation of optimum hydrophobic/hydrophilic properties, electronic conducting network and pore size and its distribution in the micro-porous layer.

One of the recent approaches to improve low temperature fuel cell performance is by using conducting PANI as a constituent in the catalyst layer for PEMFC. Mondal et al. [12] have reported the electrooxidation of ascorbic acid on anode coated with PANI catalyst and discussed its implications to fuel cells. Zabrodskiĭ et al. [13] studied carbon-supported PANI as anode catalyst in an attempt to Pt free fuel cells. Nechitalov et al. [14] used catalytic layers based on PANI and α-C-Pt composite obtained by magnetron sputtering for fuel cells whereas Michel et al. [15] reported a layer-by-layer assembly of PANI fibers based nanostructured membrane electrodes for fuel cell. Rimbu et al. [16] had reported the preparation of PANI-supported Pt 40% as the catalyst for the fuel cell and evaluated the catalytic performance by cyclic voltammetry. In spite of very good dispersion of Pt in the range of 3–5 nm on the PANI support, poor performance of PANI-supported catalyst has been reported and attributed to the possibility of chemical incorporation of Pt inside the PANI particles forming a Pt/PANI complex. Very recently, Yang et al. has fabricated a composite of Nafion®/PANI membrane and evaluated in a PEMFC without any external humidification. The proton conducting characteristics at lower RH conditions were attributed to the conjugated bonds in the PANI. As this study was for portable PEMFC applications, there is systematic variation of external humidity [17].

In direct methanol fuel cells, PANI has been used as catalyst support and also as a composite electrolyte material along with

* Corresponding author. Tel.: +1 480 727 1102; fax: +1 480 727 1723.
E-mail address: amk@asu.edu (A.M. Kannan).

0378-7753/$ – see front matter © 2009 Elsevier B.V. All rights reserved.
doi:10.1016/j.jpowsour.2009.04.002

Nafion® to reduce methanol cross over [18,19]. The Pt supported on PANI nanofibers catalyst has been reported to show higher electrochemical active surface area and higher methanol oxidation reaction activity than the Pt/C. Even though the methanol cross over reduction by two orders of magnitude has been reported, there is a reduction in proton conductivity of the composite membrane with Nafion® and SPEEKK [20]. The electrocatalytic properties of Pt incorporated PANI films have been reported by Fungaro et al. [21] for oxidation of ethanol in sulfuric acid solutions. The optimum catalytic activity for a polyaniline film of 0.08 μm thickness with Pt loading of 9.5 $\mu g\,cm^{-2}$ has been reported for ethanol concentration of 0.50 $mol\,l^{-1}$. Synthesis of nanostructured PANI/mesoporous TiO_2 composite and its use as an anode in *Escherichia coli* microbial fuel cells (MFCs) had been reported by Qiao et al. [22]. The composite with 30 wt.% PANI had given rise to the best bio- and electrocatalytic performance with a 2-fold higher power density (1495 $mW\,m^{-2}$) over the previously reported work. The use of conducting PANI in biofuel cell has also been reported by Han and Furukawa [23]. PANI-coated aluminum plates evaluated as bipolar plates have shown about an order of magnitude reduction in corrosion current with only a minor increase in contact resistance towards PEMFC applications [24]. All the above studies have attempted to use PANI as membrane constituent for PEM, methanol and ethanol fuel cells or as bipolar plate coating. There are few other studies to show that the conductivity of PANI increased about 5 times in wet conditions compared with dry state [25,26]. At high water transport, the ionic resistance of the electrolyte in fuel cell has been reported to be lower, while gas diffusion is generally hindered by the presence of high water content [27].

Based on the combined properties of high electronic conductivity at wet conditions and balanced water retaining capacity at the sites of the dopants, we propose here for the first time the use of PANI as interlayer in MEA of PEM fuel cell. The objective of the present study is to design and develop MEAs with PANI based interlayer between the catalyst-coated membrane and the GDL and to evaluate them in single cell PEMFCs under various RH conditions using H_2/O_2 for improving water management while utilizing its inherent conductivity. Conducting PANI, doped with three different acids, two organic acids such as camphor sulfonic acid (CSA) and p-toluene sulfonic acid (pTSA) and an inorganic acid, hydrochloric acid (HCl) have been used for making the interlayer. The MEAs with functionalized PANI as interlayer assisted in maintaining moisture content in the membrane and exhibited stable performance even at 50% RH at 80 °C using H_2 and O_2 at ambient pressure.

2. Experimental

2.1. Synthesis of doped PANI

PANI was synthesized by oxidative polymerization of aniline hydrochloride with ammonium peroxydisulfate at room temperature as per the procedure in the literature [26,28]. In brief, 0.2 M aniline hydrochloride was prepared and the polymerization was carried out in hydrochloric acid medium by the slow addition of the oxidant. The polymer precipitated as fine particles and the reaction product was in dispersion. The precipitate was filtered, washed with 1 M HCl and then with acetone to remove the low molecular weight oligomers followed by doping with respective dopants such as HCl, CSA and pTSA. The purpose of this study is to prepare PANI at room temperature using inorganic acid and organic acid dopants and to evaluate their role as an interlayer in GDL of PEM fuel cell at various RH conditions. The conductivity of the PANI samples was evaluated by four-probe method. The doped samples were characterized by FTIR (Thermonicolet, Avatar 360 model). The powder sample was placed on the diamond holder and thin film was formed by applying a flat surface (Smart Golden Gate accessory). The vibrational spectra features were recorded in % transmittance mode.

2.2. Gas diffusion layers

Gas diffusion layers were fabricated with a teflonized non-woven carbon paper developed by Hollingsworth & Vose Company, West Groton, MA. Teflon content in the macro-porous carbon paper substrate is about 15 wt.% to avoid flooding by the product water. Hydrophobic characteristic of the micro-porous layers was provided by TE5839 Teflon suspension (Dupont, Wilmington, DE). Vapor grown carbon fiber (VGCF-H) manufactured by Showa Denko America Inc., NY was mixed with nano-chain PUREBLACK® 205-110 Carbon (Superior Graphite Co., Chicago, IL) to provide improved mechanical strength and adhesion between the micro-porous and macro-porous layers. A slurry of carbons (75 wt.% PUREBLACK® carbon and 25 wt.% nano-fibrous carbon (VGCF)) with PTFE dispersion (25 wt.%) in isopropanol was prepared by ultrasonication followed by magnetic stirring for the fabrication of micro-porous layers used in this study.

The slurry was coated on to the non-woven carbon paper using an RDS-50 wire rod (RD Specialties, Webster, NY 14580, USA) attached to a fully automated Easy Fuel Cell Coater Combi EC10100 (Coatema Coating Machinery GmbH, Dormagen, Germany). The carbon loading of the micro-porous layer was controlled by the slurry composition (10 wt.% carbon in isopropyl alcohol) and the wire thickness on the wire rod. The gap between the wires on the wire rod determined the amount of carbon material during the coating process. The carbon substrate was fixed in place and the wire rod was driven at a speed of 4 $m\,min^{-1}$. Subsequently, carbon paper with the micro-porous layer was dried at room temperature and then sintered at 350 °C for 30 min. The carbon loading for the micro-porous layer was ~2.8 $mg\,cm^{-2}$ with RDS-50 wire rod. Wetting characteristics of the GDL samples were evaluated by NRL CA Goniometer (Rame-hart 100). The contact angle of a droplet of water and ethanol mixture (1:1 ratio) on the micro-porous layer was measured after 1 min.

2.3. Doped polyaniline interlayer

In order to improve low RH performance of the PEMFC, MEA was designed to an interlayer between the catalyst layer and the micro-porous layer of the GDL. A schematic representation of the MEA in Fig. 1 shows the doped PANI interlayer between the catalyst

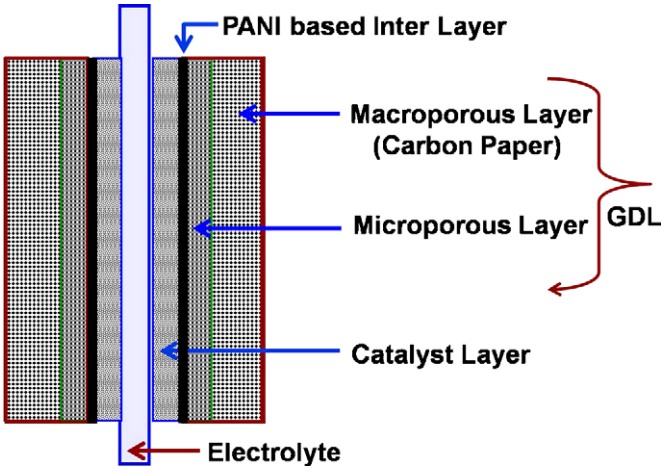

Fig. 1. Schematic representation of MEA showing the PANI based interlayer between the catalyst layer and micro-porous layer of the GDL on anode and cathode side (relative dimensions are not to scale).

Table 1
Electrical conductivity of PANI samples at room temperature.

Sample	Dopant	Electrical conductivity ($S\,cm^{-1}$)
1	Camphor sulfonic acid	2.28×10^{-1}
2	p-Toluene sulonic acid	1.29
3	Hydrochloric acid	1.00×10^{-2}

Camphor sulfonic acid: C_6H_7 $(CH_3)_2CH_2$ SO_3H; p-toluene sulfonic acid: $CH_3C_6H_4SO_3H$.

layer and the micro-porous layer of the GDL, both on the anode and cathode sides, respectively. Slurries of the PANI-CSA, PANI-HCl and PANI-pTSA in isopropanol (5 wt.%) were sprayed on the surface of the micro-porous layer. For comparison purpose, pristine GDLs were also evaluated in various RH conditions.

2.4. Catalyst deposition on membrane

Catalyst-coated membranes (CCM) were fabricated as follows. Catalyst ink was prepared by adding isopropanol (20 ml for 1 g of electrocatalyst) after purging the Pt/C catalyst powder (TKK, Japan) in flowing nitrogen gas for about 30 min to avoid any flame/ignition. In order to extend the reaction zone of the catalyst layer, 5% Nafion® (Ion Power Inc., New Castle, DE, USA) solution (10 ml Nafion® solution for 1 g of electrocatalyst) was added to the catalyst slurry. Catalyst coatings on Nafion® membrane (NRE 212, Ion Power Inc., New Castle, DE, USA) with 5 cm^2 active area were fabricated as anode and cathode, respectively, by spraying Pt/C catalyst ink using the micro-spray method. The catalyst loadings on the anode and cathode catalyst layers were about 0.5 and 1 mg Pt cm^{-2}, respectively. The catalyst-coated Nafion®-212 membrane was vacuum dried at about 50 °C for 30 min before assembling them in the fuel cell test cell.

2.5. Membrane electrode assembly and fuel cell evaluation

The MEAs were fabricated by sandwiching the GDLs with doped PANI interlayer and the CCM inside the single cell test cell (Fuel Cell Technologies Inc., Albuquerque, NM, USA). Gas sealing was achieved using silicone-coated fabric gasket (Product #CF1007, Saint-Gobain Performance Plastics, USA) and with a uniform torque of 0.45 kg m^{-1}. The single cell fuel cell performance was evaluated at 80 °C at 100, 90, 80, 70, 60 and 50% RH conditions on both anode and cathode sides using Greenlight Test Station (G50 Fuel Cell System, Hydrogenics, Vancouver, Canada). Initial conditioning of the MEA was carried out at 0.4 V for 3 h at 80 °C, 100% RH. The galvanostatic polarization was done at high RH conditions first after a stabilization period of half an hour before the measurements at each RH condition. The flow rates were fixed at 200 and 400 SCCM for H_2 and O_2, respectively. Higher flow rate of O_2 was considered as an extreme situation of product water removal along with exit gas. The steady state voltage values were collected by holding the cell at each current density values for 20 s.

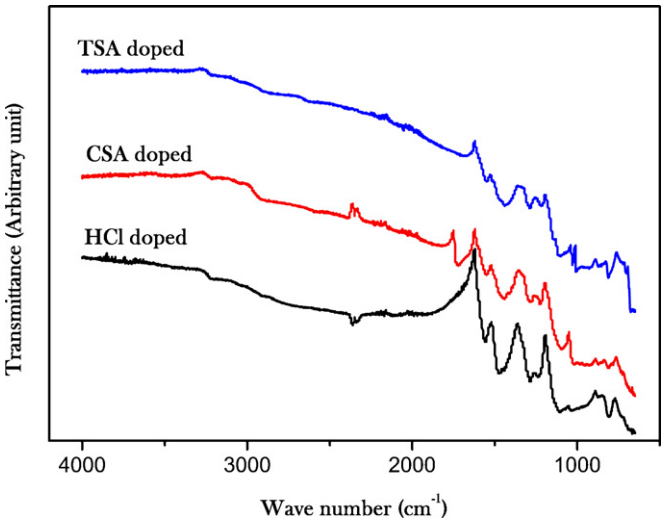

Fig. 2. FTIR data for PANI samples with various dopants CSA, HCl and pTSA.

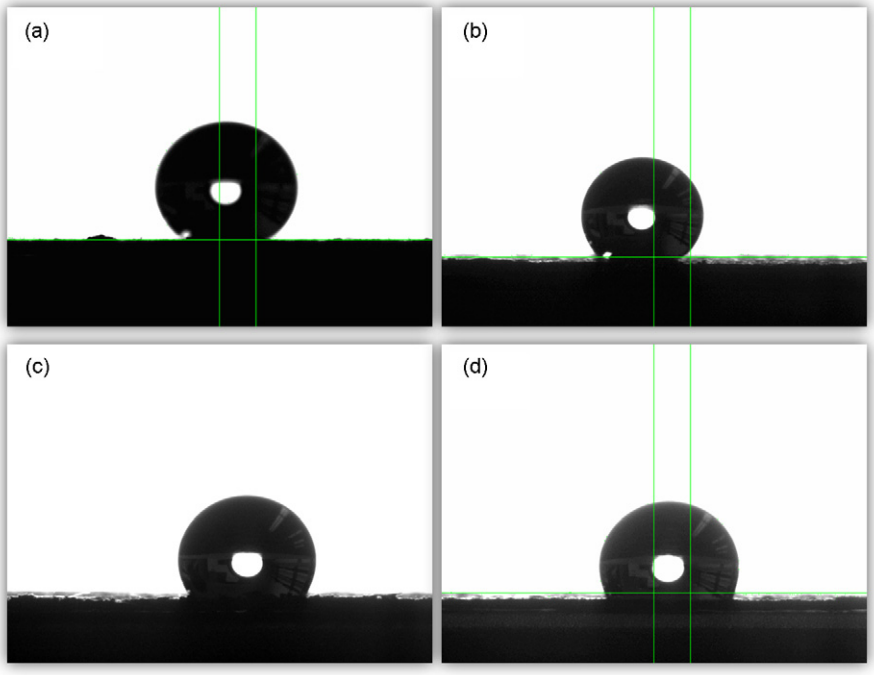

Fig. 3. Wetting angle images of (a) pristine and (b) PANI-CSA, (c) PANI-HCl and (d) PANI-pTSA coated micro-porous layers.

Table 2
FTIR spectral bands of PANI and their assignment.

Band (cm^{-1})	Assignment
1493	Benzenoid unit
1599	Quinoid band
1400–1240	C—N stretching region
1385	Presence of conjugation
1706	N—H stretching band
1114, 618	Charge delocalization peaks
1160	In-plane C—H bending mode of aromatic ring
816	Out of plane C—H bending mode

3. Results and discussion

The conductivity of the PANI samples is listed in Table 1. The functional groups of the doped PANI samples as analyzed by FTIR spectroscopy are labeled in the % transmittance mode in Fig. 2, while their band and peak assignments are summarized in Table 2. Presence of the characteristics bands of PANI in all the three samples matching with the literature confirmed the formation of the polymer in each preparation [29,30].

Wetting angle images for pristine and doped PANI (PANI-pTSA, PANI-HCl and PANI-CSA) based micro-porous layers of the GDL using water–ethanol (1:1 ratio) drop are shown in Fig. 3(a–d). Ethanol was mixed with water to improve the wetting characteristics, as pure water alone could not be used for wetting angle measurements. The wetting angle is the angle that the tangent makes with the point of contact of the drop with the surface under study. The surface characteristics and its constituents influence this property. The wetting angle values measured by the Goniometer are 140, 114, 110 and 101 degrees for pristine, PANI-pTSA, PANI-HCl and PANI-CSA, based micro-porous layers, respectively. Obviously, an MEA with interlayer that gives rise to relatively lower wetting angle is expected to perform better in the fuel cell at lower RH conditions. The Scanning Electron Micrographs of the GDL surface with the doped PANI samples are shown in Fig. 4 along with that of the pristine surface. PANI prepared under identical conditions but

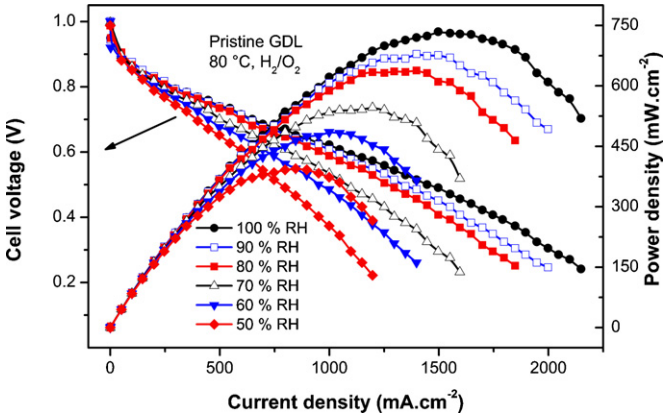

Fig. 5. Fuel cell performance of an MEA using pristine GDLs (without interlayer) at 80 °C using H_2/O_2 at ambient pressure at various RH conditions.

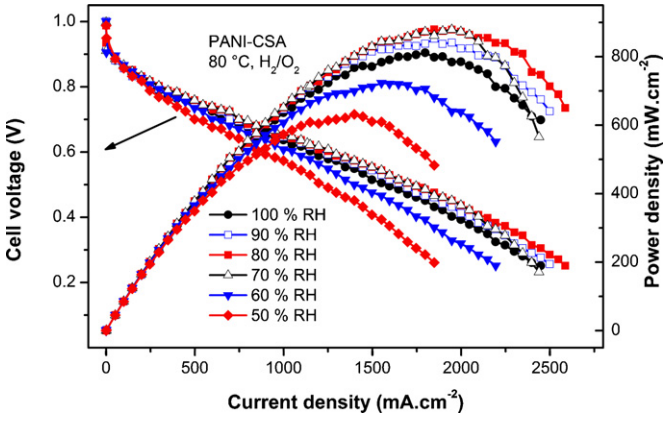

Fig. 6. Fuel cell performance of an MEA with PANI-CSA based interlayer at 80 °C using H_2/O_2 at ambient pressure at various RH conditions.

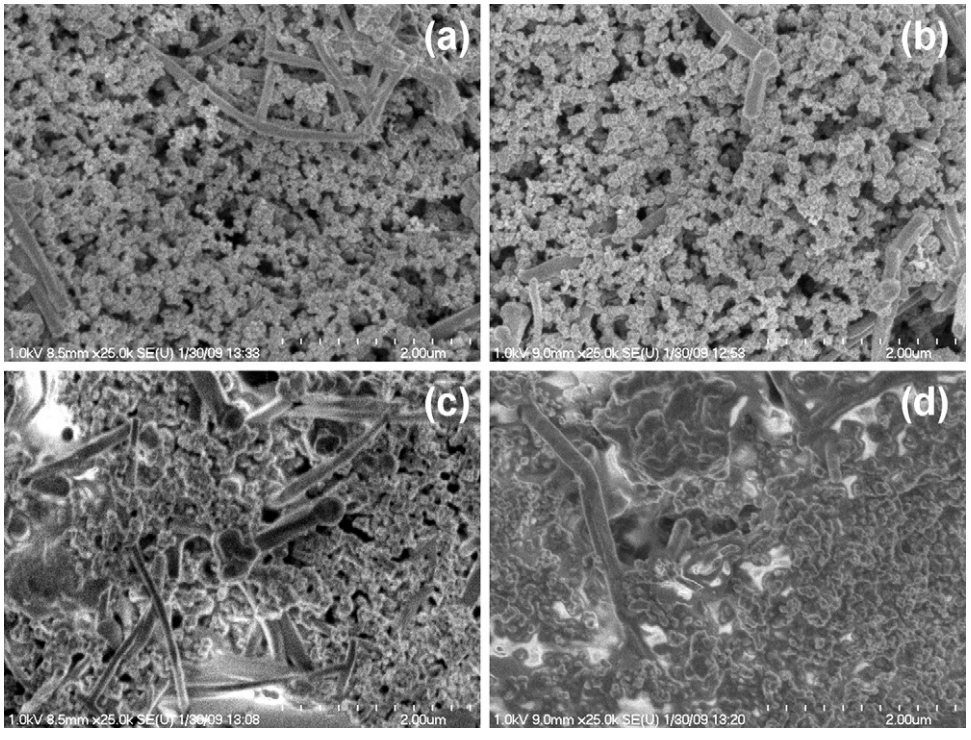

Fig. 4. Scanning Electron Micrographs of (a) pristine and (b) PANI-CSA, (c) PANI-HCl and (d) PANI-pTSA coated micro-porous layers.

treated with different dopants show different morphology due to the stereochemistry of the functional groups. All the samples show the assembly of the nano particles of PANI with high porosity and good depth profile in the case of PANI-CSA followed by PANI-HCl and PANI-TSA. Evidently, the change in surface structure of the doped PANI layer on the surface of the micro-porous layers could lead to holding the product water especially during the low RH conditions of the fuel cells.

Fig. 5 compares the fuel cell performance of an MEA using pristine GDLs (without interlayer) at 80 °C using H_2/O_2 at ambient pressure at various RH conditions. Fig. 6 shows the fuel cell performance of an MEA with PANI-CSA based interlayer at 80 °C using H_2/O_2 at ambient pressure at various RH conditions. Comparison for Figs. 5 and 6 highlight the consistent and superior performance of the PANI-CSA based system with high power density at all RH conditions. It is interesting to note that the MEA with PANI-CSA interlayer shows a peak power density of 600 mW cm^{-2} at 50% RH compared to that with pristine GDLs (~370 mW cm^{-2}).

In order to highlight the performance of various doped PANI interlayer based MEAs, fuel cell performance data were consolidated at specific RH conditions. Fig. 7(a–f) compares the fuel cell performance data at 80 °C using H_2/O_2 at various RH conditions (100, 90, 80, 70, 60 and 50% RH) at ambient pressure for MEAs with and without doped PANI based interlayers. The diminishing performance of the pristine GDL is well evident from Fig. 7(a–f) with decreasing RH conditions. PANI-CSA shows consistent high performance at all RH conditions. The lower wetting angle value for the PANI-CSA interlayer (see Fig. 3) compared to all other samples is responsible for the highest performance at lower RH conditions, by retaining the product water to maintain the electrolyte moist enough to keep the ionic conductivity. As seen from Fig. 7(a and b), the PANI-pTSA interlayer based MEAs showed the maximum

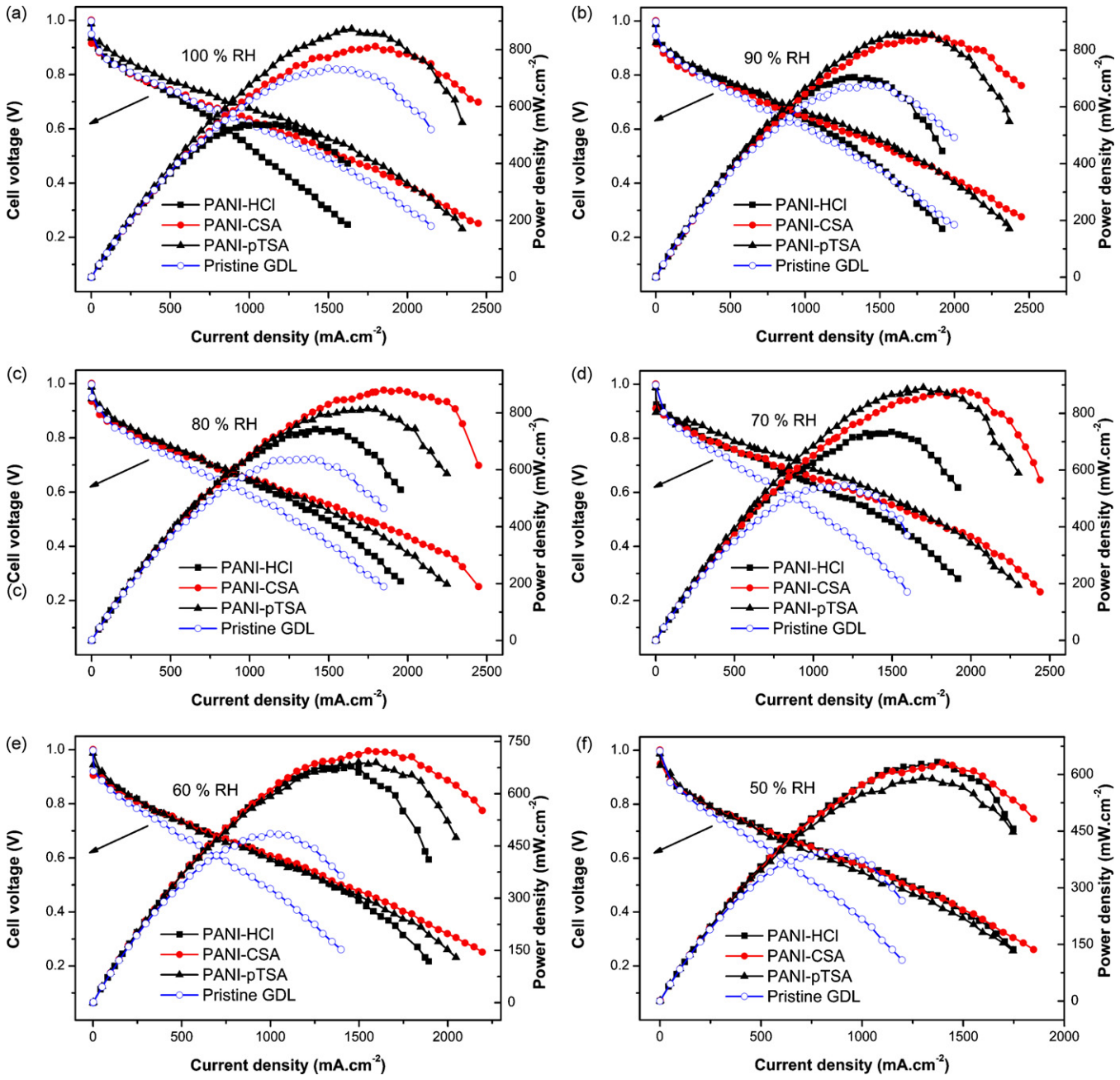

Fig. 7. Fuel cell performance comparison of MEAs with and without doped PANI based interlayers at (a) 100, (b) 90, (c) 80, (d) 70, (e) 60 and (f) 50% RH conditions using H_2/O_2 at ambient pressure.

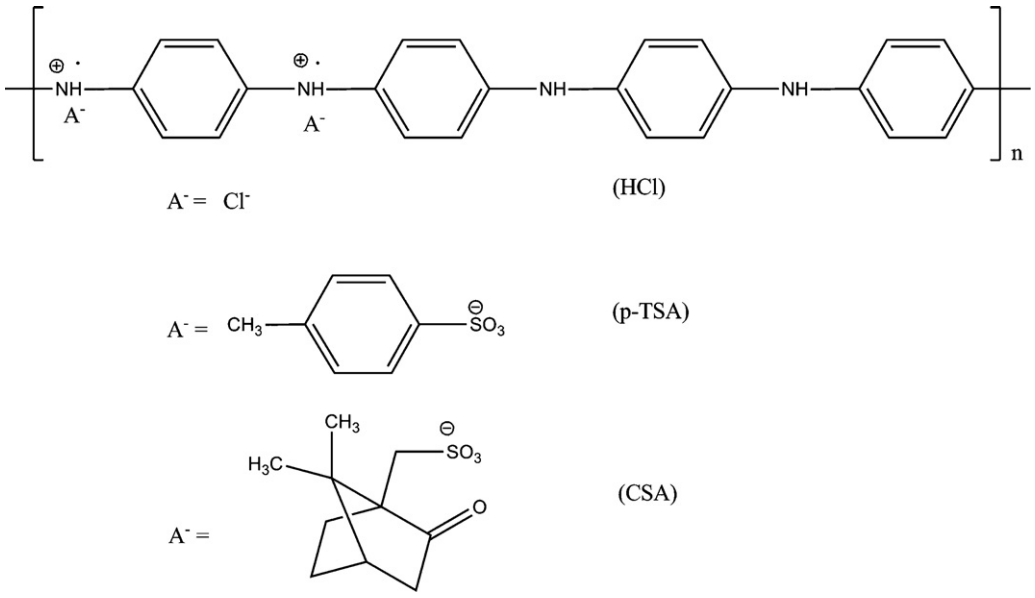

Fig. 8. Chemical structure of doped PANI.

peak power density values compared to other MEAs. This could be due to the relatively higher wetting angle value avoiding electrodes flooding. However, the PANI-CSA interlayer based MEAs showed the maximum peak power density values at lower RH conditions. This could be attributed to the lowest wetting angle value keeping the electrolyte moist at lower RH values (say 50 and 60%).

As evident from Fig. 7(f) the performance of all the PANI based systems is almost identical and far higher than that of the pristine GDL, at the lowest RH condition (50%) evaluated in the present study. The structure of the conducting doped PANI samples as shown in Fig. 8 helps in understanding the improved performance of the PANI-CSA system. The extended conjugation of the aromatic backbone takes care of the conductivity of the PANI samples irrespective of the RH conditions and the spatial separation of the functional group in the doped PANI samples provides the delinked channel for the water flow. While in the pristine GDL water flows through the available channels, in the cases of PANI interlayer water can flow only in contact with the hydrophilic sites, the functional groups. Of the three functional groups, CSA provides a spatial hydrophilic anisotropy away from the conjugated backbone facilitating water drain by effective hopping of the water dipole at the sulfonic acid functional group by hydrogen bonding. In the case of PANI-HCl sample, the spatial delinking of the water flow is very poor and under high RH conditions, the water dipole may also be influenced by the π electron delocalization of the backbone. In the case of PANI-TSA, though spatial delinking of the water flow is possible, it is affected by the extended conjugation of the toluene ring and hence shows relatively lower performance than that of PANI-CSA system at high RH conditions. PANI-CSA system has a decoupled water flow channel and electronic conducting pathway making the system smart in water management. Further research study of the quantitative comparison between the functional group density per unit volume (and hence the number of moles of water draining through it) of doped PANI and the capillary transport will throw more light.

4. Conclusions

An MEA configuration with doped PANI based interlayer between the catalyst layer and micro-porous layer of the GDL was designed, developed and evaluated in PEMFC at lower RH conditions. All the doped PANI interlayer based MEAS exhibited enhanced fuel cell performance at low RH conditions, while the PANI-CSA showed the maximum fuel cell performance at all RH conditions. The improved water management is attributed to the balanced hydrophilicity of the interlayer. The aromatic backbone of the conducting doped PANI provides the hydrophobicity and the functionalization by the dopants provides the sites for water transport by hydrogen bonding. The spatial hydrophilic anisotropy in PANI-CSA facilitates smart water management at all RH conditions. At high current densities the higher water concentration in the interlayer creates positive pressure to flush out water through the GDL on the cathode side. On the anode side, the humidity held at the functional groups of doped PANI avoids membrane drying even at low RH conditions and thus favor high performance in the cases of all the doped PANI.

Acknowledgement

Cindrella Louis and Arunachala Kannan acknowledge the financial support from the Arizona State University through Global Engagement Seed Grant for inter-institutional research collaboration.

References

[1] M.V. Williams, H. Russell Kunz, J.M. Fenton, J. Power Sources 135 (2004) 122–134.
[2] A.M. Kannan, L. Cindrella, L. Munukutla, Electrochim. Acta 53 (2008) 2416–2422.
[3] J. Mirzazadeh, E. Saievar-Iranizad, L. Nahavandi, J. Power Sources 131 (2004) 194–199.
[4] C. Lim, C.Y. Wang, Electrochim. Acta 49 (2004) 4149–4156.
[5] G. Park, Y. Sohn, T. Yang, Y. Yoon, W. Lee, C. Kim, J. Power Sources 131 (2004) 182–187.
[6] S. Shimpalee, U. Beuscher, J.W. Van Zee, Electrochim. Acta 52 (2007) 6748–6754.
[7] M. Han, S.H. Chan, S.P. Jiang, J. Power Sources 159 (2006) 1005–1014.
[8] A.M. Kannan, A. Menghal, I. Barsukov, Electrochem. Comm. 8 (2006) 887.
[9] E. Antolini, R.R. Passos, E.A. Ticianelli, J. Power Sources 109 (2002) 477–482.
[10] X.L. Wang, H.M. Zhang, J.L. Zhang, H.F. Xu, Z.Q. Tian, J. Chen, H.X. Zhong, M. Liang, B.L. Yi, Electrochim. Acta 51 (2006) 4909–4915.
[11] X. Wang, H. Zhang, J. Zhang, H. Xua, X. Zhua, J. Chena, B. Yi, J. Power Sources 162 (2006) 474–479.
[12] S.K. Mondal, R.K. Raman, A.K. Shukla, N. Munichandraiah, J. Power Sources 145 (2005) 16–20.
[13] A.G. Zabrodskiĭ, M.E. Kompan, V.G. Malyshkin, I.Y. Sapurina, J. Tech. Phys. Lett. 32 (2006) 758–761.
[14] A. Nechitalov, E. Astrova, D. Goryachev, T. Zvonareva, V. Ivanov-Omski, A. Remenyuk, I. Sapurina, O. Sreseli, V. Tolmachev, Tech. Phys. Lett. 33 (2007) 545–547.

[15] M. Michel, F. Ettingshausen, F. Scheibam, A. Wolz, C. Roth, J. Phys. Chem. Chem. Phys. 10 (2008) 3796–3801.
[16] G.A. Rimbu, C.L. Jacksona, K. Scott, J. Optoelectron. Adv. Mater. 8 (2006) 611–616.
[17] J. Yang, P.K. Shen, J. Varcoe, Z. Wei, J. Power Sources 189 (2009) 1016–1019.
[18] Z. Chen, L. Xu, W. Li, M. Waje, Y. Yan, Nanotechnology 17 (2006) 5254–5259.
[19] C. Chih-Yuan, I.G. Jairo, C.D. Mikel, F.D.C. Roni, L.D. Andrew, C.D.C. Joao, J. Power Sources 166 (2007) 324–330.
[20] X. Li, D. Chen, D. Xu, C. Zhao, Z. Wang, H. Lu, H. Na, J. Membr. Sci. 275 (2006) 134–140.
[21] D.A. Fungaro, A. Oliveira-Neto, M. Linardi, Latin Am. Appl. Res. 37 (2007) 223–226.
[22] Y. Qiao, S. Bao, C. Ming, L.X. Cui, Z. Lu, J. Guo, ACS Nano 2 (2008) 113–119.
[23] Y. Han, Y. Furukawa, Int. J. Green Energy 3 (2006) 17–23.
[24] S. Joseph, J.C. McClure, P.J. Sebastian, J. Moreira, E. Valenzuela, J. Power Sources 177 (2008) 161–166.
[25] S.P. Armes, J.F. Miller, Synth. Met. 22 (1988) 385–393.
[26] J. Heeger, J. Phys. Chem. B 105 (2001) 8475–8491.
[27] P. Staiti, Z. Poltarzewski, V. Alderucci, G. Maggio, N. Giordano, A. Fasulo, J. Appl. Electrochem. 22 (1992) 663–667.
[28] J. Stejskal, R.G. Gilbert, Pure Appl. Chem. 74 (2002) 857–867.
[29] L. Zhang, M. Wan, Nanotechnology 13 (2002) 750–755.
[30] F.A. Beleze, A.J.G. Zarbin, J. Braz. Chem. Soc. 12 (2001) 542–547.